ESC HEART FAILURE
ESC Heart Failure (2022)
Published online in Wiley Online Library (wileyonlinelibrary.com) **DOI:** 10.1002/ehf2.14234

ORIGINAL ARTICLE

Lumican accumulates with fibrillar collagen in fibrosis in hypertrophic cardiomyopathy

Chloe Rixon[1,2]*, Kristine Andreassen[1,2,3], Xin Shen[1,2], Pugazendhi Murugan Erusappan[1,2], Vibeke Marie Almaas[3], Sheryl Palmero[1,2], Christen Peder Dahl[4], Thor Ueland[4,5,6], Ivar Sjaastad[1,2], William Edward Louch[1,2], Mathis Korseberg Stokke[1,2,3], Theis Tønnessen[1,7], Geir Christensen[1,2] and Ida Gjervold Lunde[1,2]

[1]*Institute for Experimental Medical Research, Oslo University Hospital Ullevål and University of Oslo, Oslo, Norway;* [2]*K.G. Jebsen Centre for Cardiac Research, University of Oslo, Oslo, Norway;* [3]*Department of Cardiology, Oslo University Hospital, Rikshospitalet, Oslo, Norway;* [4]*Research Institute of Internal Medicine, Oslo University Hospital, Rikshospitalet, Oslo, Norway;* [5]*Institute of Clinical Medicine, University of Oslo, Oslo, Norway;* [6]*K. G. Jebsen Thrombosis Research and Expertise Center, University of Tromsø, Tromsø, Norway; and* [7]*Department of Cardiothoracic Surgery, Division of Cardiovascular and Pulmonary Diseases, Oslo University Hospital Ullevål, Oslo, Norway*

Abstract

Aims Familial hypertrophic cardiomyopathy (HCM) is the most common form of inherited cardiac disease. It is characterized by myocardial hypertrophy and diastolic dysfunction, and can lead to severe heart failure, arrhythmias, and sudden cardiac death. Cardiac fibrosis, defined by excessive accumulation of extracellular matrix (ECM) components, is central to the pathophysiology of HCM. The ECM proteoglycan lumican is increased during heart failure and cardiac fibrosis, including HCM, yet its role in HCM remains unknown. We provide an in-depth assessment of lumican in clinical and experimental HCM.

Methods Left ventricular (LV) myectomy specimens were collected from patients with hypertrophic obstructive cardiomyopathy (n = 15), and controls from hearts deemed unsuitable for transplantation (n = 8). Hearts were harvested from a mouse model of HCM; *Myh6* R403Q mice administered cyclosporine A and wild-type littermates (n = 8–10). LV tissues were analysed for mRNA and protein expression. Patient myectomy or mouse mid-ventricular sections were imaged using confocal microscopy, direct stochastic optical reconstruction microscopy (dSTORM), or electron microscopy. Human foetal cardiac fibroblasts (hfCFBs) were treated with recombinant human lumican (n = 3) and examined using confocal microscopy.

Results Lumican mRNA was increased threefold in HCM patients ($P < 0.05$) and correlated strongly with expression of collagen I (R^2 = 0.60, $P < 0.01$) and III (R^2 = 0.58, $P < 0.01$). Lumican protein was increased by 40% in patients with HCM ($P < 0.01$) and correlated with total (R^2 = 0.28, P = 0.05) and interstitial (R^2 = 0.30, $P < 0.05$) fibrosis. In mice with HCM, lumican mRNA increased fourfold ($P < 0.001$), and lumican protein increased 20-fold ($P < 0.001$) in insoluble ECM lysates. Lumican and fibrillar collagen were located together throughout fibrotic areas in HCM patient tissue, with increased co-localization measured in patients and mice with HCM (patients: +19%, $P < 0.01$; mice: +13%, $P < 0.01$). dSTORM super-resolution microscopy was utilized to image interstitial ECM which had yet to undergo overt fibrotic remodelling. In these interstitial areas, collagen I deposits located closer to (−15 nm, $P < 0.05$), overlapped more frequently with (+7.3%, $P < 0.05$) and to a larger degree with (+5.6%, $P < 0.05$) lumican in HCM. Collagen fibrils in such deposits were visualized using electron microscopy. The effect of lumican on collagen fibre formation was demonstrated by adding lumican to hfCFB cultures, resulting in thicker (+53.8 nm, $P < 0.001$), longer (+345.9 nm, $P < 0.001$), and fewer (−8.9%, $P < 0.001$) collagen fibres.

Conclusions The ECM proteoglycan lumican is increased in HCM and co-localizes with fibrillar collagen throughout areas of fibrosis in HCM. Our data suggest that lumican may promote formation of thicker collagen fibres in HCM.

Keywords Heart; HCM; SLRPs; Extracellular matrix; ECM remodelling; dSTORM

Received: 23 May 2022; Revised: 6 October 2022; Accepted: 7 November 2022
**Correspondence to: Chloe Rixon, Institute for Experimental Medical Research, Oslo University Hospital, Ullevål, PB 4956 Nydalen, NO-0424 Oslo, Norway.*
Email: chloe.rixon@medisin.uio.no

Introduction

Familial hypertrophic cardiomyopathy (HCM) is the most common inherited cardiac disease, affecting 1:500 of the global population.[1] In HCM, cardiomyocyte sarcomere gene variants lead to increased left ventricle (LV) wall thickness, attributed to cardiomyocyte hypertrophy and disarray, inflammation, and accumulation of fibrosis.[1,2] Such adverse remodelling causes heart failure, with diastolic dysfunction, arrhythmias, and increased risk of sudden cardiac death.[2,3] Fibrosis is becoming increasingly recognized as a critical pathophysiological process in HCM, correlating with adverse clinical outcomes and present in most patients with HCM.[4,5]

Cardiac fibrosis is characterized by the excessive production of extracellular matrix (ECM), where structural fibrillar collagens I and III are deposited by activated cardiac fibroblasts in focal areas of cardiomyocyte death (replacement fibrosis), between cardiomyocytes (interstitial fibrosis) and around vessels (perivascular fibrosis).[6] Not only the quantity but also the quality of the remodelled matrix affects the progression of heart failure.[7,8] The quality of the cardiac ECM is mainly determined by the organization of its components, of which fibrillar collagen I is most abundant. Therefore, examining molecules that may govern fibrillar collagen organization in fibrosis, such as the ECM proteoglycans, is an important step in identifying routes for anti-fibrotic therapy in HCM patients.

The small leucine-rich proteoglycans (SLRPs) constitute a family of secreted, glycosylated proteins with distinct roles in the cardiac ECM, including collagen organization.[9] The SLRP lumican, specifically, is increased in patients with heart failure[10,11] and is shown to be important for heart failure progression and survival during studies of lumican knockout mice.[12,13] Moreover, lumican was found to be one of the most regulated proteins in HCM, and studies in non-cardiac tissues indicate a role for lumican in development of fibrosis.[11,14–16] Despite this, lumican has not yet been examined in HCM in detail at the molecular level. Therefore, we have studied the production and localization of lumican in myectomy samples from patients with HOCM, hearts from the well-established *Myh6* R403Q mouse model of HCM and human foetal cardiac fibroblasts (hfCFBs) treated with lumican, with special focus on relationship to collagen.

Methods

Ethics

The human biopsy protocol was approved by the Regional Committee for Medical Research Ethics (REK ID S-02295 and S-05172) and the South-Eastern Regional Health Authority of Norway and conformed with the principles outlined in the Declaration of Helsinki. Informed consent was provided by patients and next of kin of heart donors. Mouse protocols were approved by the Norwegian National Animal Research Committee and the Norwegian Food Safety Authority (FOTS ID 7466 and 17235) and conformed to the Animals in Research: Reporting In Vivo Experiments (ARRIVE) Guidelines.[17]

HOCM patients and myectomy samples

LV biopsies were obtained during septal myectomy from HOCM patients (n = 15) which had been referred for septal reduction therapy at Oslo University Hospital (OUH). Tissue samples were snap-frozen in liquid nitrogen and stored at −80°C. For cryosections, a small number of flash-frozen samples were embedded at a later time-point using OCT-COMPOUND (Chemi-Teknik AS, Oslo, Norway). LV tissue from non-diseased hearts considered for transplantation but deemed unsuitable served as controls (initial n = 10), with two samples excluded from further analyses due to degraded tissue/poor quality (final n = 8).

HOCM patient characteristics for samples used in qPCR and WB analyses were described previously.[6] In brief, the diagnostic criteria were LV wall thickness >15 mm with other causes of hypertrophy excluded, with non-dilated LV and EF ≥ 50%. Indication for septal reducing therapy was the presence of symptoms despite optimal medical treatment, significant blood flow obstruction in LV outflow tract with peak gradient >30–50 mmHg, and basal septal wall thickness >15 mm. Histological examination of fibrosis was performed by an experienced pathologist.[6] Blood sampling was performed at the time of septal myectomy to measure circulating collagen peptides in serum: the amino terminal peptide of type I procollagen (PINP), the amino terminal peptide of type III procollagen (PIIINP), and the carboxy-terminal telopeptide of type I collagen (ICTP).

Mouse model of HCM

Mice were 129SvEv background (Taconic). Comparisons were made between animals heterozygous for the alpha myosin heavy chain 6 R403Q mutation ($\alpha MHC^{403/+}$) and wild-type littermates. This well-established and extensively characterized genetic mouse model of HCM exhibits an accelerated phenotype upon administering cyclosporine A (CsA).[18–20] A total of 36 mice were used in this study (n = 8–10).

Male mice aged 7.6–10.0 weeks received CsA or vehicle (Veh) for 3 weeks. CsA was administered orally to achieve continuous dosage. Each mouse received 40 g of chow soaked for 24 h in a 10 mL mixture of 0.0375% 100 mg/mL CsA (Sandimmun Neoral Mixture, NOVARTIS) in sesame oil (ACROS Organics, Thermo Fisher), replaced once per week.

Transthoracic echocardiography was performed under light isoflurane (1.7%) anaesthesia at baseline and prior to organ harvest. Echocardiograms were performed by an experienced researcher blinded to genotype and treatment. Measurements were made of the interventricular septum (IVS), LV posterior wall (LVPW), LV inner dimension (LVID), and left atrial diameter (LAD), as previously described.[21] Anaesthesia time was 5–10 min per mouse. Images were analysed by a single blinded, independent observer.

Mice were weighed prior to harvest to collect body weight (BW). To harvest mice, mice were anaesthetized with isoflurane (4%), and the heart and lungs excised. Excised tissues were washed in ice-cold PBS. Lung weights (LW) and whole heart weights (HW) were collected. A transverse mid-ventricular cut through the heart was performed and pieces washed in ice-cold PBS. The basal half was snap-frozen in 2-methylbutane using embedding matrix, OCT-COMPOUND (Chemi-Teknik AS, Oslo, Norway) for cryosections, and the apical half, containing tissue from both the septum and posterior wall, was directly snap-frozen for individually matched molecular biology analyses.[22] After harvesting tissues, hind limbs were excised above the knee and tissue removed to measure tibia length (TL). Frozen mouse tissues were pulverized using a Multisample Biopulverizer (12-well, BioSpec Products, #59012MS) prior to RNA or protein isolation.

Human foetal cardiac fibroblasts

hCFBs (#306-05f, Cell Applications Inc., CA) at Passage 5 were cultured for 5 days with 2 μg/mL recombinant human lumican protein (#2846-LU carrier-free, R&D) or vehicle (dPBS) added at Day 0. Concentration of recombinant lumican was based on previous studies.[14,23,24] Immunohistochemistry was performed for lumican and collagen I (see *Data S1* for further description). Entire coverslips were scanned at 20× using an AxioScan Z1 (Carl Zeiss) and 63× Z-stack confocal images of 2–3 μm thickness were obtained using an LSM800 Airyscan (Leica) microscope. Three biological replicates were performed. Seven randomly selected images were quantified using CT Fire (see *Data S1* for further description).

Gene expression

RNA was isolated and qPCR performed using frozen tissue as described previously.[10] Frozen mouse LV tissue was homogenized in QIAzol Lysis Reagent (Qiagen) using the TissueLyser system (Qiagen). RNA extraction was performed with the miRNeasy RNA isolation kit (#217084, Qiagen). RNA concentration was measured using a Multiskan Sky Microplate Spectrophotometer (Thermo Fisher). cDNA was synthesized using an iScript™ cDNA Synthesis Kit (Bio-Rad). TaqMan™ assays (Applied Biosystems, Thermo Fisher) were used for qPCR. Human TaqMan assays: *RPL32* Hs00851655_g1; *LUM* Hs00929860_m1; *COL1A2* Hs01028956_m1; *COL3A1* Hs00943809_m1. Mouse TaqMan assays: *Rpl32* Mm02528467_g1; *Lum* Mm01248292_m1; *Col1a1* Mm00801666_g1; *Col1a2* Mm00483888_m1; *Col3a1* Mm00802331_m1; *Lox* Mm00495386_m1; *Tgfb1* Mm01178820_m1; *Postn* Mm01284919_m1; *Ctgf* Mm01192932_g1; *Nppa* Mm01255747_g1; *Nppb* Mm01255770_g1; and *Myh7* Mm00600555_m1. *RPL32* and *Rpl32* were used as reference genes.

Immunoblotting

Protein was isolated from human and mouse LV biopsies. Proteins from patient biopsies were isolated prior to this study using a PBS-based lysis buffer (1% Triton X-100/0.1% Tween-20/PBS), yielding total lysates containing cellular plus soluble/loosely bound ECM proteins. From mouse LV tissue, proteins were separated into two protein lysates; a cellular plus soluble/loosely bound ECM fraction (cell + sol. ECM) and an ECM-enriched fraction, containing tightly ECM-bound and insoluble ECM proteins (insol. ECM). The cell + sol. ECM fraction was isolated through homogenization in a PBS-based lysis buffer (1% Triton X-100/0.1% Tween-20/PBS) and the insol. ECM fraction isolated from the remaining insoluble pellet with 1% SDS lysis buffer.[25]

Immunoblotting was performed as previously described[10,13,26] using 5% BSA/TBS-T blocking solution and 1:500 goat anti-human lumican antibody (R&D AF2846) or goat anti-mouse lumican antibody (R&D AF2745). Deglycosylation of lumican was performed using PNGaseF as previously described.[13,26] Blots were developed with the Azure 600 imaging system (Azure Biosystems, CA) and automated quantification performed with AzureSpot software. Total protein was used as loading control (Coomassie blue for patient tissues; Revert 700 Total Protein Stain #926-11011 LI-COR for mouse tissues). Glycosylated lumican was detected at 50–75 kDa, omitting the non-specific band at approximately 75–80 kDa, as previously described.[13] Deglycosylated lumican (i.e. the remaining core protein after deglycosylation) was detected at 38 kDa as previously described[13] and was used as a measure of total lumican protein levels.

Confocal microscopy

All imaging was performed on 7 μm cryosections on poly-L-lysine coated slides (Poly-Prep, Sigma-Aldrich) maintained at −20°C during cutting and stored at −80°C prior to fixation. Cryosections were fixed and immunohistochemistry was performed for lumican and collagen I (see *Data S1* for further de-

scription). Negative antibody controls were performed in patient tissues (*Figure S1A*), mouse tissues (*Figure S1B*) and cell cultures (*Figure S1C*).

Confocal imaging was performed with a 63× objective on an LSM800 Airyscan (Leica) microscope before scanning the entire section using an AxioScan Z1 (Carl Zeiss). Type of fibrosis identified was based on previous definition in the HOCM patient cohort.[6] Quantification was performed using Fiji/ImageJ or QuPath software using scans of entire sections for quantification of lumican signal (mean signal intensity, normalized to background signal via F/F0). Representative images were chosen based on visual representation of quantified data.

dSTORM super-resolution imaging

All dSTORM imaging was performed on 4 μm cryosections. Cryosections were fixed and immunohistochemistry performed for lumican and collagen I (see *Data S1* for further description). Imaging was performed using a 63× objective on an LSM710/Elyra microscope (Leica). The blinded operator selected interstitial areas where lumican and collagen were present, then acquired lumican signal emission at 647 nm wavelength and collagen signal at 555 nm wavelength with dSTORM.

Resulting images were processed, thresholded to remove intracellular signal and analysed using a custom Python script to group collagen and lumican deposits in each image. 'Deposits' were defined by localization, with the assumption that, if a group of pixels viewed via dSTORM did not have a gap distinguishable at 25 nm resolution, then they likely corresponded to proteins interacting in the ECM. Defining a group of proteins as a single deposit enabled quantification of deposit characteristics (overlap, inter-deposit distance). Additional analyses were performed using Fiji/ImageJ (see *Data S1* for further description). 3D dSTORM images were rendered using ParaView software.

Electron microscopy (EM)

Mouse hearts were excised, 1 mm mid-ventricular sections cut using a razor blade, fixed and processed before cutting 100 nm ultrathin sections for imaging via transmission electron microscopy (TEM) (see *Data S1* for further description).

Statistics

GraphPad Prism 9 was used for statistical comparisons. All single comparisons were performed using a Student's *t*-test and evaluated for Gaussian distribution of residuals. If the *F*-test displayed significant difference between variances, Student's *t*-test with Welch's correction was used. If normality of residuals tests were failed (alpha = 0.05), the Mann–Whitney *U* test was used instead. When comparisons were between multiple variables, one-way ANOVA with Tukey post hoc analysis was applied. Where variances were significantly different, Brown–Forsythe and Welch ANOVA with Dunnett's T3 was used, and where normality tests failed, Kruskal–Wallis test with Dunn's multiple comparisons used. Correlations were analysed via simple linear regression.

Results

Lumican is increased in the myocardium of HOCM patients

Lumican levels were increased in myectomy specimens from HOCM patients vs. controls. Lumican mRNA levels were threefold higher in HOCM (*Figure 1A*). Immunostaining sections for lumican protein (*Figures 1B* and *S1D*) showed a 35% increase in signal in HOCM (*Figure 1C*). Immunoblotting revealed a twofold increase in 50–75 kDa glycosylated lumican protein levels in HOCM (*Figure 1D, i* and *iii*, complete blots *Figure S2A*). Deglycosylation of these samples to total lumican protein level at 38 kDa displayed a 1.4-fold increase (*Figure 1D, ii* and *iv*, complete blots *Figure S2B*). Lumican deposition was evident across areas of replacement, interstitial and perivascular fibrosis (*Figure 1E*, white arrowhead indicating fibrosis).

Lumican co-localizes with collagen I in fibrotic regions of the HOCM myocardium

Confirming cardiac fibrosis in HOCM patients, collagen I expression (measured via *COL1A2*) was increased 3.6-fold and collagen III expression (measured via *COL3A1*) was increased 2.9-fold in HOCM (*Figure 2A*). *LUM* mRNA levels correlated positively with *COL1A2* (R^2 = 0.60) and *COL3A1* (R^2 = 0.58), displaying positive covariance between increased collagen and lumican in HOCM (*Figure 2B*). Similarly, total lumican protein levels in myocardial specimens were positively correlated with total and interstitial fibrosis determined by histological examination (*Figure 2C*). Despite this, total lumican protein was not correlated with circulating collagen biomarkers PINP (*Figure S3A*, left panel), ICTP (*Figure S3A*, right panel), nor PIIINP (*Figure S3B*). Co-staining HOCM and control sections for collagen I and lumican demonstrated increased co-localization in HOCM (*Figure 2D*), quantified as a 3.5-fold increase (*Figure 2E*). Qualitative assessment of lumican and collagen I revealed that lumican spread pervasively throughout fibrotic areas and was often found localized closely to collagen I (*Figure 2F*, white arrows indicating typical lumican and collagen I localization).

Figure 1 Lumican is increased in the myocardium of HOCM patients. Left ventricular (LV) myectomy samples were obtained from HOCM patients and compared with LV samples from control hearts (Ctrl). (A) Patient lumican (LUM) mRNA expression relative to control (n = 3 Ctrl, n = 14 HOCM). (B) Cryosections were immunostained for lumican (green) and scanned at 20×, from control (left) and HOCM (right) tissues. Negative antibody control displayed in *Figure S1A*. Scale bars have a width of 1 mm. (C) Quantification of lumican protein via mean signal intensity in control and HOCM tissue sections (n = 3 Ctrl, n = 3 HOCM). (D) Immunoblotting of total lysates for lumican protein in control and HOCM tissues, displaying lumican in its 50–75 kDa glycosylated state (blot displayed in *i* and quantified as 'glycosylated' in *iii*). These samples were deglycosylated using PNGaseF to measure total lumican protein via the 38-kDa core protein (blot displayed in *ii* and quantified as 'deglycosylated' in *iv*). Representative bands are shown, with complete blots and loading controls displayed in *Figure S2*. Schematic of the small leucine-rich proteoglycan lumican is displayed with its four N-glycan sites where keratan sulfate glycosaminoglycan (GAG) modification can occur. Scissors indicate the removal of N-glycans, and hence, GAG chains with PNGaseF. (E) Representative images from HOCM patient tissues displaying lumican in replacement (left panel), interstitial (centre-left panel) and perivascular (centre-right panel) fibrosis, with control tissue (right panel) for comparison. White arrowheads display lumican in the relevant area. WGA (magenta) displays remaining ECM proteins and outlines cardiomyocytes, whereas DAPI (light blue) displays nuclei. Scale bars indicate a width of 250 μm. Data are presented as means ± SD with individual points; statistical comparisons were performed by t-test. $^{*}P < 0.05$, $^{**}P < 0.01$.

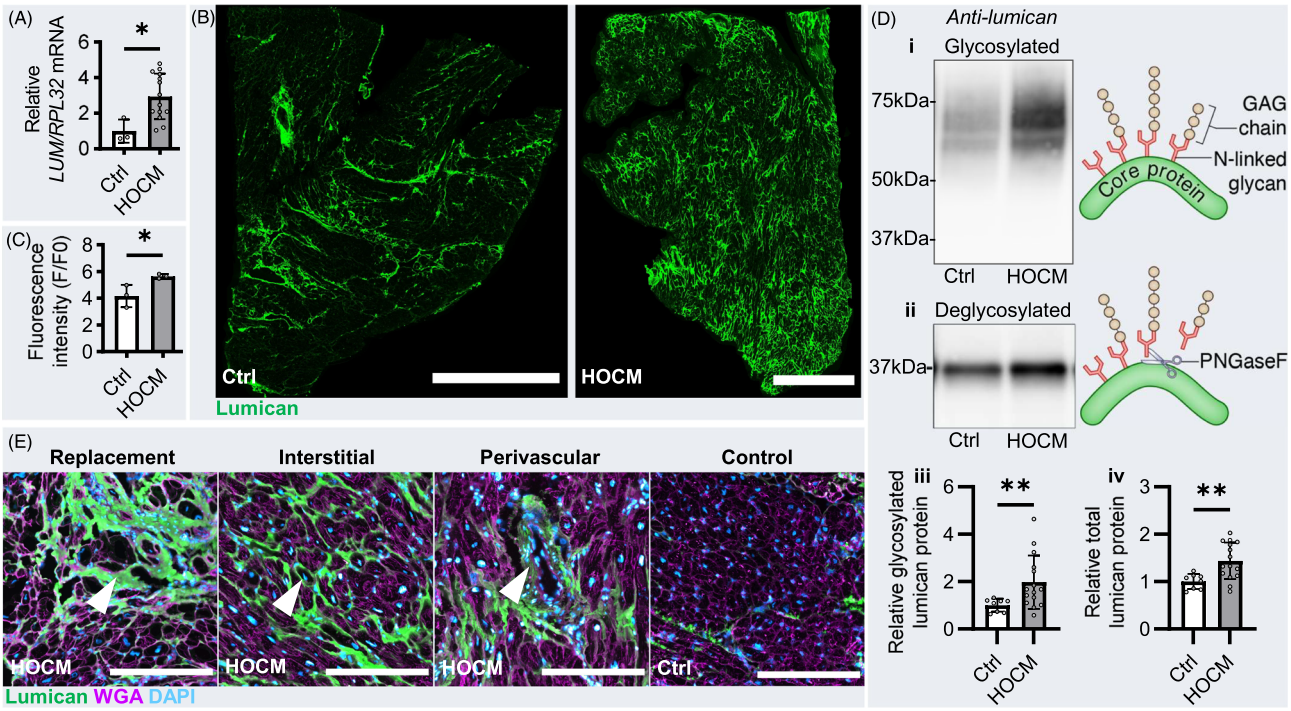

Lumican and collagen are upregulated and localized across the left ventricles of mice with HCM

Patient samples were limited and collected from regional biopsies. Thus, to assess fibrotic remodelling across the entire LV, we utilized the *Myh6* R403Q mouse model where HCM develops in response to CsA treatment.[18–20]

Echocardiography, organ weights and gene expression profiles after CsA treatment confirmed the expected HCM phenotype in *Myh6* R403Q mice vs. WT Veh controls (*Table 1*). Increased HW, HW/TL ratio, LVPW during diastole (LVPW;d), and expression of pathological molecular markers (including *Myh7*) indicated hypertrophic remodelling (*Table 1*), most notably in the posterior wall, as observed previously in this model.[18,19,22] Hypercontractility was evident by increased fractional shortening (FS) (*Table 1*). Pulmonary congestion and congestive heart failure were indicated by increased LW, LW/TL ratio, LAD, and expression of heart failure biomarkers *Nppa* and *Nppb* (*Table 1*). Increased expression of fibrillar collagens I (*Col1a1*, *Col1a2*) and III (*Col3a1*) by 6.7- to 8.6-fold indicated expected levels of fibrosis (*Figure 3A*). Accordingly, expression of the collagen cross-linking enzyme lysyl oxidase (*Lox*) was increased by 6.2-fold (*Figure 3B*). Expression of *Tgfb1*, *Ctgf*, and *Postn* were increased, indicating increased TGF-β activity (*Table 1*).

Lum mRNA was upregulated 4.2-fold in HCM mice vs WT Veh controls (*Figure 3C*). Immunoblotting for LV lumican protein showed that lumican protein from cell + sol. ECM lysates increased threefold, whereas lumican protein from insol. ECM lysates (containing tightly ECM-bound and insoluble ECM proteins) increased 20-fold in HCM (*Figure 3D*, complete

Figure 2 Lumican co-localizes with collagen I in fibrotic regions of the HOCM myocardium. Correlation and co-localization between lumican and collagen I were examined in left ventricular (LV) myectomy samples from HOCM patients and compared with control hearts (Ctrl). (A) mRNA expression levels of collagen types I and III were analysed via *COL1A2* (left) and *COL3A1* (right), shown relative to control (n = 5 Ctrl, n = 14 HOCM). (B) Correlations (R^2) for collagen I or III mRNA expression with lumican mRNA expression in HOCM samples (n = 14). (C) Levels of total lumican protein via Western blotting correlated against fibrosis (%), quantified via histological examination of HOCM patient myectomy tissues (n = 14) by an experienced pathologist. Total fibrosis percentage in the tissue is displayed (left panel), with interstitial fibrosis (right panel) correlated separately. R^2 and P values displayed within the graph. (D) Cryosections were binarized to assess degree of red/green overlap through Fiji/ImageJ (n = 3 Ctrl, n = 3 HOCM, lumican in green, collagen I in red, and overlap in yellow). Scale bars have a width of 1 mm and representative images follow Pearson's R quantification. (E) Pearson's R value describes degree of overlap between red and green wavelengths of emission as indicated by the yellow areas (values 0–1 = 0–100% overlap). (F) Representative confocal images displaying typical presentation of lumican (green) and collagen I (red) in control vs. HOCM tissues. White arrows indicate where lumican and collagen are found together. Negative antibody control displayed in *Figure S1A*. Scale bars indicate a width of 25 μm. WGA (cyan) displays the remaining ECM and outlines cardiomyocytes. DAPI (light blue) displays nuclei. Data are presented as means ± SD with individual points; statistical comparisons were performed via linear regression or t-test. $^*P < 0.05$, $^{**}P < 0.01$, $^{***}P < 0.001$.

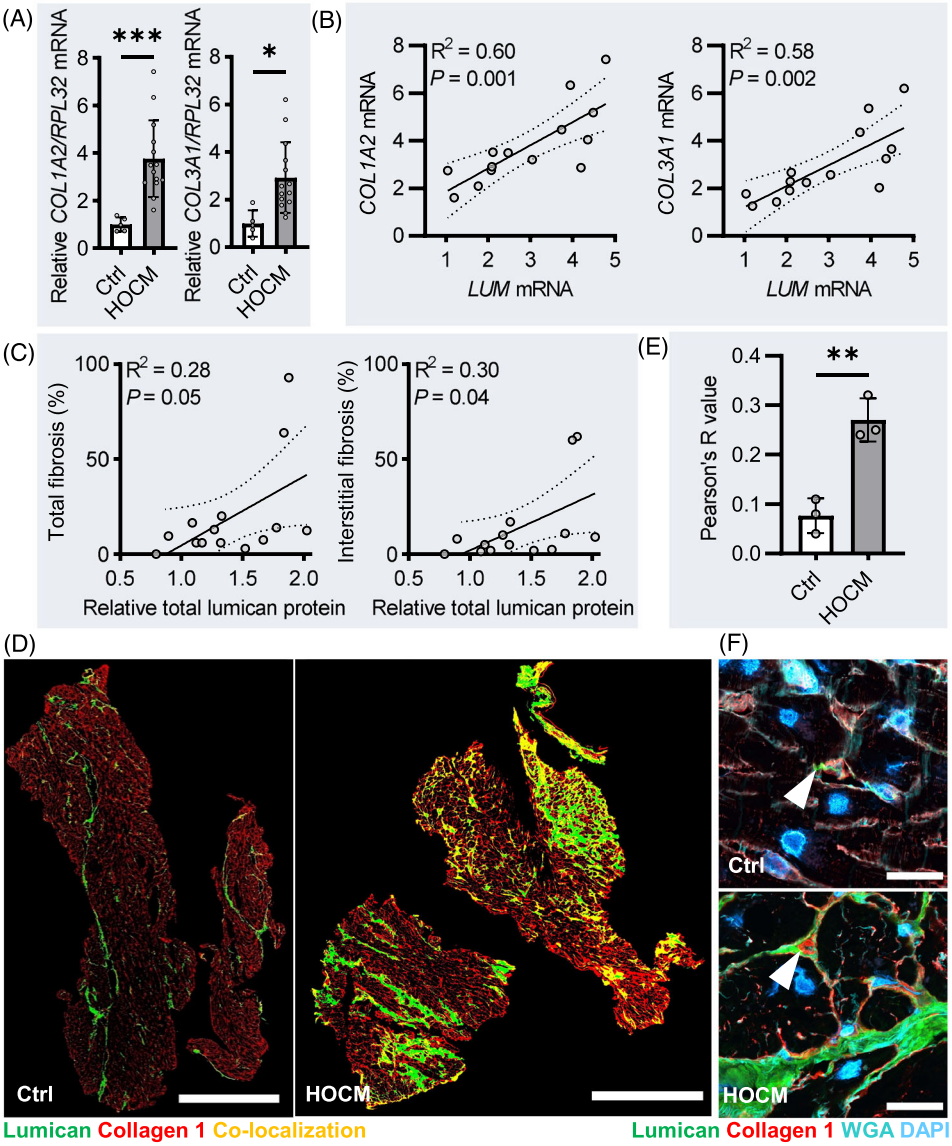

Table 1 HCM phenotype of *Myh6* R403Q mice using CsA induction

	WT		*Myh6* R403Q	
Treatment	Veh	CsA	Veh	CsA
N	9	8	9	10
Biometric data at harvest				
Age (weeks)	11.8 ± 0.9	11.8 ± 0.8	11.8 ± 0.9	11.7 ± 0.9
BW (g)	22.7 ± 2.1	20.2 ± 2.1*	22.8 ± 2.5	18.2 ± 2.5***
TL (mm)	17.1 ± 0.4	17.2 ± 0.4	17.1 ± 0.3	17.0 ± 0.5
HW (mg)	122.1 ± 19.0	118.7 ± 19.2	117.4 ± 17.2	137.6 ± 19.4*
HW/TL (mg/mm)	7.1 ± 1.0	6.9 ± 1.2	6.8 ± 0.9	8.1 ± 1.1$^{\#}$
LW (mg)	145.4 ± 20.2	144.6 ± 10.9	143.7 ± 16.7	216.0 ± 62.3**$^{\#\#}$
LW/TL (mg/mm)	8.5 ± 1.1	8.4 ± 0.6	8.4 ± 0.9	12.7 ± 3.8**$^{\#\#}$
M-mode echocardiography				
LAD (mm)	2.16 ± 0.29	2.33 ± 0.49	2.26 ± 0.26	2.87 ± 0.63*
LVPW;d (mm)	0.65 ± 0.10	0.70 ± 0.11	0.82 ± 0.11	1.23 ± 0.48**$^{\#\#}$
IVS;d (mm)	0.77 ± 0.15	0.70 ± 0.13	0.76 ± 0.10	0.71 ± 0.19
LVID;d (mm)	4.01 ± 0.40	3.78 ± 0.47	3.80 ± 0.57	3.05 ± 0.76**$^{\#}$
FS (%)	16.9 ± 5.4	20.5 ± 7.1	27.7 ± 8.7*	33.7 ± 13.3**$^{\#}$
Relative LV mRNA expression (qPCR)				
Nppa/Rpl32	1.0 ± 0.6$^{\#}$	3.5 ± 1.4*	2.7 ± 1.7	21.3 ± 4.4***
Nppb/Rpl32	1.0 ± 0.1	1.2 ± 0.5	1.3 ± 0.9	2.0 ± 0.5**
Myh7/Rpl32	1.0 ± 0.4	0.7 ± 0.4	1.7 ± 0.6$^{\#}$	3.1 ± 1.6**$^{\#\#\#}$
Tgfb1/Rpl32	1.0 ± 0.3	1.3 ± 0.2	1.0 ± 0.3	1.9 ± 0.3***$^{\#\#\#}$
Ctgf/Rpl32	1.0 ± 1.4	0.8 ± 0.3	1.0 ± 1.3	1.9 ± 0.6*$^{\#}$
Postn/Rpl32	1.0 ± 0.3	2.2 ± 0.7	2.7 ± 1.9	15.1 ± 4.1***$^{\#}$
Rpl32	1.0 ± 0.1	1.0 ± 0.1	1.1 ± 0.1	1.0 ± 0.2

BW, body weight; FS, fractional shortening; HW, heart weight; IVS;d, interventricular septal end diastole; LAD, left atrial diameter; LVID;d, left ventricular internal dimension end diastole, LVPW;d, left ventricular posterior wall end diastole; LW, lung weight; TL tibia length.
Biometric data, M-mode echocardiography and left ventricular (LV) mRNA expression characteristics (means ± SD) of heterozygous *Myh6* R403Q and wild-type (WT) male mice subjected to 3 weeks of cyclosporine A (CsA) or vehicle (Veh) treatment. mRNA expression data shown relative to WT Veh average. Statistical comparisons were performed by one-way ANOVA, the Kruskal–Wallis test, or Brown-Forsythe and Welch, as appropriate; for treatment group vs, WT Veh $^{*}P < 0.05$, $^{**}P < 0.01$, $^{***}P < 0.001$; vs. WT CsA $^{\#}P < 0.05$, $^{\#\#}P < 0.01$, $^{\#\#\#}P < 0.001$.

blots *Figure S4*). Immunohistochemistry revealed lumican deposition across the LV increased by 36% in HCM (*Figure 3E*). Co-staining for lumican and collagen revealed that co-localization increased by 13% in HCM (*Figure 3F*).

Lumican and collagen I in areas with and without apparent fibrosis in HCM

Confocal imaging in control mouse tissues revealed lumican deposition was mostly restricted to areas between sheets of healthy cardiomyocytes. (*Figure 4A*, green arrow), whereas collagen surrounded cardiomyocytes in a thin layer (*Figure 4A*, red arrow). Similar patterning could be observed in HCM mouse tissues in areas that had not yet undergone fibrotic remodelling, which we termed 'without apparent fibrosis' (*Figure 4B*, pink arrow). Observations in entire scans of the LV revealed that lumican remodelled in parallel with degree of fibrosis, from 'unapparent' to severe (*Figure 4B*, white dashed arrow). Using confocal microscopy, we visualized lumican clearly in areas that appeared to be at the very beginning of fibrotic remodelling (*Figure 4C*, left panel, white arrow) and in areas with severe fibrotic remodelling (*Figure 4C*, right panel). This led us to examine whether we could observe subtle alterations in lumican and collagen deposition in areas as yet without overt fibrotic remodelling.

Collagen I deposits reach larger sizes more frequently and co-localize more with lumican in areas without apparent fibrosis in HCM

Examining alterations in areas without overt remodelling presented a novel challenge, due to the subtle nature of the remodelling we wished to observe. Therefore, we applied dSTORM to obtain images of lumican and collagen down to 25 nm resolution in interstitial ECM areas without apparent fibrosis (*Figure 5A*). Binarizing these images enabled definition of protein deposits and establishment of where they overlapped (*Figure 5B*). Even in areas without apparent fibrosis, collagen deposits reached a larger size more frequently in HCM, indicating early or low levels of fibrotic remodelling (*Figure 5C*). We used EM to directly visualize such collagen deposits, displaying how collagen fibrils collect to form larger structures in healthy tissue (*Figure 5D*, upper panel), in areas without apparent fibrosis (*Figure 5D*, centre panel) or with overt fibrosis (*Figure 5D*, lower panel). Quantifying inter-deposit distances in these interstitial areas via dSTORM revealed that collagen deposits localized more closely to lumican in HCM (*Figure 5E*). Collagen deposits also overlapped with lumican more frequently (*Figure 5F*, left panel) and to a greater extent (*Figure 5F*, right panel) in HCM. This co-localization was visualized via 3D dSTORM reconstruction in control (*Figure S5*) and HCM (*Figure S6*).

Figure 3 Lumican and collagen are upregulated and localized across left ventricles of mice with HCM. Heterozygous *Myh6* R403Q and wild-type (WT) littermate male mice were subjected to 3 weeks of cyclosporine A (CsA) or vehicle (Veh) administration (n = 8–10). *Myh6* R403Q mice have an accelerated phenotype upon treatment with CsA. (A) mRNA expression levels of collagens I (*Col1a1*, left, *Col1a2*, centre) and III (*Col3a1*, right) shown relative to WT Veh control. (B) mRNA expression levels of collagen cross-linking enzyme lysyl oxidase *(Lox)* shown relative to WT Veh control. (C) mRNA expression levels of lumican *(Lum)* normalized to *Rpl32* and relative to WT Veh control. (D) Lumican protein in its native 50–75 kDa glycosylated form as detected in two protein lysate fractions; left lane = cellular, membrane and soluble/loosely bound ECM fraction (cell + sol. ECM); right lane = ECM-enriched fraction containing insoluble ECM protein (insol. ECM). Representative bands shown, complete blots and loading controls displayed in *Figure S4*. Quantification was performed between 50 and 75 kDa, shown relative to WT Veh control. (E) Lumican protein localization across the LV displayed in transverse, mid-ventricular cryosections from control (WT Veh, left) and HCM (*Myh6* R403Q CsA, right) mice, quantified using mean signal intensity of lumican protein (n = 5 Ctrl, n = 5 HCM). Representative images shown. Negative antibody control displayed in *Figure S1B*. Scale bars indicate a width of 1 mm. (F) Sections were digitally processed to only contain the LV when measuring co-localization (n = 5 Ctrl, n = 5 HCM), showing lumican (green) and collagen I (red) staining with overlap (yellow) measured via Pearson's R (values 0–1 = 0–100% overlap). Representative images shown. Scale bars indicate a width of 1 mm. All data are given as means ± SD; multiple statistical comparisons performed as appropriate by one-way ANOVA, the Kruskal–Wallis test or Brown–Forsythe and Welch vs. WT Veh; single comparisons made by t-test. $^{*}P < 0.05$, $^{**}P < 0.01$, $^{***}P < 0.001$.

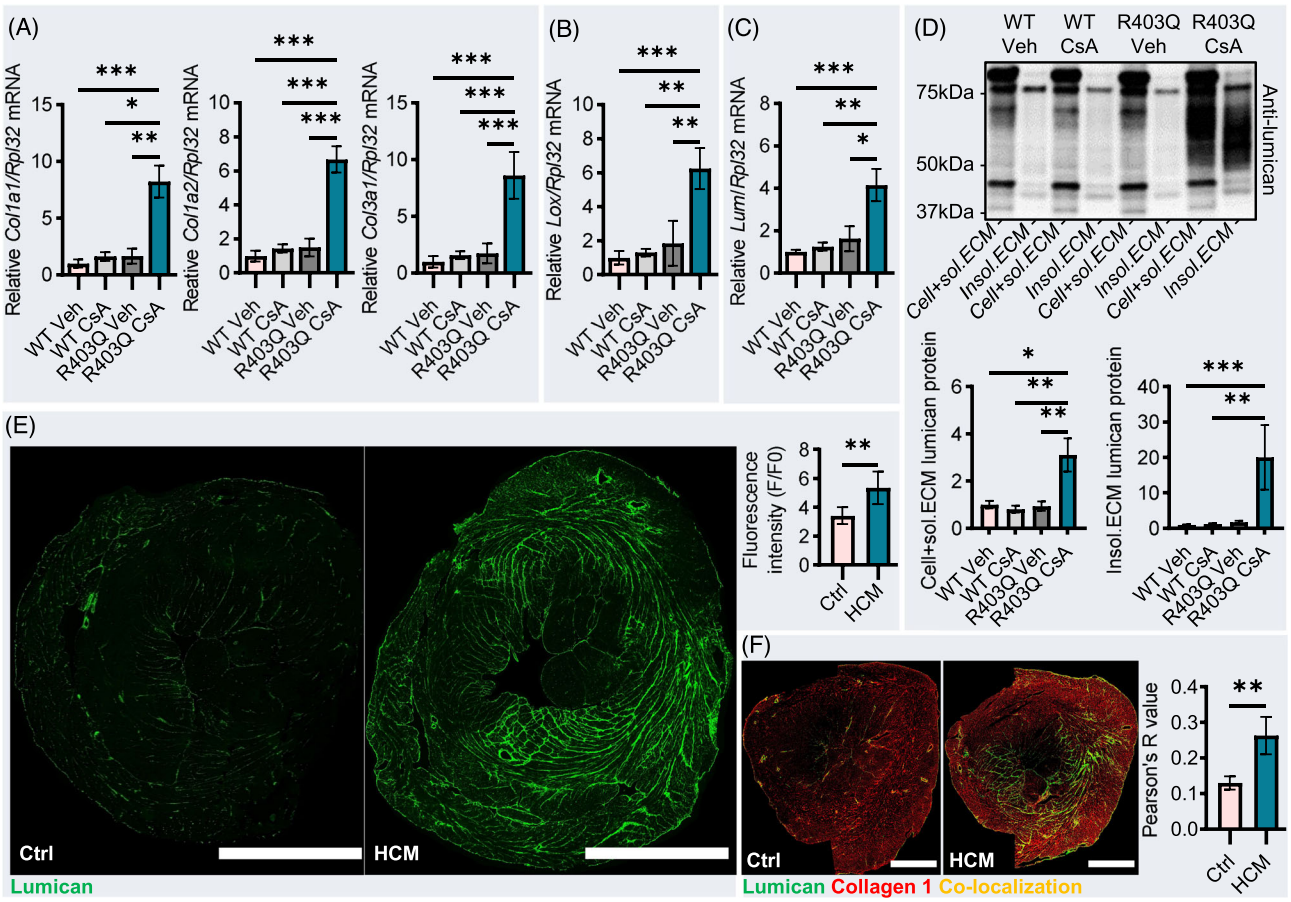

Exogenous lumican increases collagen fibre width in cultured human foetal cardiac fibroblasts

To investigate whether the co-localization of lumican to areas of collagen accumulation indicates a causal role in the accumulation process, we added recombinant human lumican to hfCFBs cultured for 5 days. Recombinant lumican was integrated into the ECM and co-localized with collagen I (*Figure 6A*), resulting in formation of thicker (*Figure 6B*) and longer (*Figure 6C*) collagen fibres. Collagen fibres were found to be fewer in number in cultures with lumican (*Figure 6D*). As fibres in cultures with lumican were larger, yet fewer, this suggests that lumican may promote formation of thicker collagen fibres via accumulation of collagen.

Figure 4 Lumican and collagen I in areas with and without apparent fibrosis in HCM. Confocal imaging of lumican and collagen I deposition in heterozygous *Myh6* R403Q and wild-type (WT) littermate male mice administered 3 weeks of cyclosporine A (CsA) or vehicle (Veh). Transverse mid-ventricular sections were used for imaging, where Ctrl = WT Veh (n = 5), HCM = *Myh6* R403Q with CsA (n = 5). Negative antibody control displayed in *Figure S1B*. (A) Representative image displaying typical organization of lumican (green) and collagen I (red) in the ECM in control. Cardiomyocytes are outlined with collagen 1 and WGA. The scale bar indicates a width of 25 μm. (B) Representative image of lumican and collagen I distribution across an HCM mouse LV, following progressive fibrotic remodelling (white dashed arrow indicates increase in severity of fibrosis from left to right). The pink arrow displays an area of HCM tissue that resembles control tissue, which is defined as an area 'without apparent fibrosis' for the purposes of this study. The scale bar indicates a width of 100 μm. (C) Representative images from HCM mouse LV displaying lumican deposition between cardiomyocytes in areas with either little (left panel, white arrow) or extensive (right panel) fibrotic remodelling. The scale bar indicates a width of 25 μm. WGA (cyan) displays remaining ECM proteins and outlines cardiomyocytes, whereas DAPI (light blue) displays nuclei.

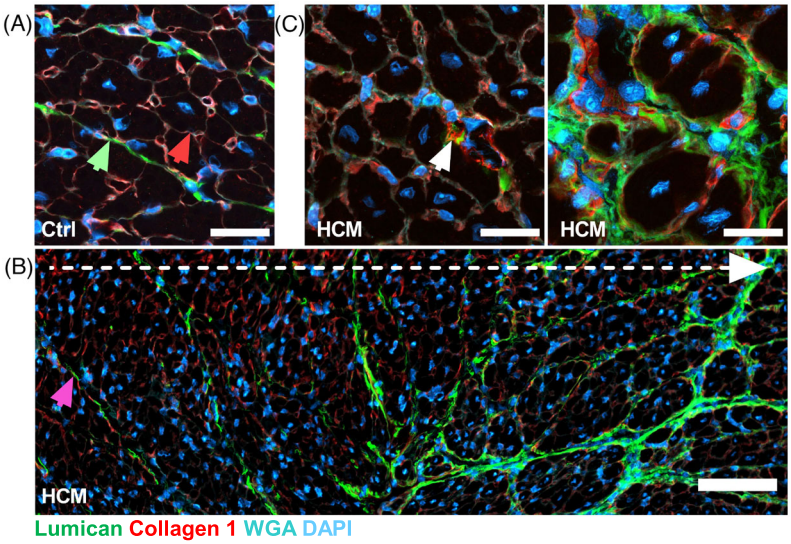

Discussion

In the present study, we demonstrate that the ECM proteoglycan lumican co-localizes with fibrillar collagen I in fibrotic areas of the myocardium in both patients and mice with HCM. Using a novel application of dSTORM, we reveal that this relationship extends even to sites of subtle fibrotic remodelling, suggesting that lumican is broadly located in any area where collagen accumulates. Importantly, we show that adding lumican to cardiac fibroblasts results in the formation of thicker and longer, yet fewer, collagen fibres, suggesting that lumican directly influences collagen accumulation in the fibrotic setting during HCM. These findings provide the first in-depth report of lumican in HCM at a molecular level.

Previous studies have associated levels of cardiac lumican with fibrosis in heart disease.[10,13,26–28] In HCM, a proteomic analysis of the HOCM patient myocardium found lumican to be among the most upregulated proteins.[11] In the aforementioned study, correlation of lumican with diagnostic parameters showed that increased myocardial lumican was associated with amount of fibrosis and diastolic dysfunction via magnetic resonance imaging.[11] In our data, we show that levels of myocardial lumican protein correlate with total and interstitial fibrosis, as measured by histology. Our results display localization of lumican to the fibrotic ECM, across any type of fibrosis, which increases in proportion with fibrotic remodelling. Seen together with previously published reports, this correlation and co-localization of increased lumican protein with fibrillar collagen indicates that lumican's role in HCM is likely to be through regulation of collagen. Such a role is consistent with previous understanding of lumican, as lumican has been shown to affect collagen in connective tissues[29] and has the ability to bind directly to collagen I with high affinity.[30,31]

The accumulation of collagen and, hence, fibrosis around dysfunctional cardiomyocytes is a common delineator for patients presenting with HCM, regardless of which sarcomere gene variant causes their HCM phenotype. Novel therapeutics for HCM, such as the myosin inhibitor mavacamten, act to reduce hypercontractility of cardiomyocytes, yet do not specifically target or reverse existing fibrosis in patients with an overt phenotype.[22,32] As the remaining fibrotic ECM alone can induce an HCM phenotype in healthy cardiomyocytes,[33] it is unlikely that therapeutic strategies for HCM will reach their full potential until we improve our understanding of molecular mechanisms of fibrosis. To approach mechanistic

Figure 5 Collagen I deposits reach larger sizes more frequently and co-localize more with lumican in areas without apparent fibrosis in HCM. Super-resolution imaging via dSTORM and electron microscopy (EM) of lumican and collagen I in *Myh6* R403Q CsA and wild-type (WT) littermate male mice administered 3 weeks of cyclosporine A (CsA) or vehicle (Veh). Transverse mid-ventricular sections were used for imaging, where Ctrl = WT Veh (n = 3), HCM = *Myh6* R403Q with CsA (n = 3). (A) Lumican (green) and collagen I (red) in confocal images of the LV (box labelled 1), with control (Ctrl) tissue in upper panels and HCM tissue in lower panels. Interstitial areas without apparent fibrosis were selected for dSTORM imaging (dashed box, labelled 2). Cardiomyocyte indicated by CM. Negative antibody control displayed in *Figure S1B*. The scale bar indicates a width of 10 μm on the left (confocal) and 5 μm on the right (dSTORM). (B) Binarized dSTORM images of lumican and collagen deposits (dotted box, labelled 3) and overlap between them (yellow). The scale bar indicates a width of 0.5 μm. (C) Frequencies of collagen deposits above 1 μm^2 are displayed via histogram for HCM (teal) and control (superimposed, pink). Collagen deposits between 0 and 1 μm^2 are not shown due to equally high numbers in both control and HCM tissues. (D) EM in control and HCM mouse LVs was performed to give direct visualization of collagen fibrils (white arrows) across different areas of fibrotic remodelling, displaying how fibrils can collect to form larger fibre structures. Representative images were selected based on dSTORM quantification. The scale bar indicates a width of 1 μm (E) The average distance from one collagen deposit to the nearest lumican deposit. (F) The number of collagen deposits that overlapped with a lumican deposit, displayed as a percentage (left panel). The degree collagen overlapped with lumican, calculated using Mander's coefficient M2 (right panel). All data presented as means ± SD; and statistical comparisons performed by *t*-test. * $P < 0.05$, ** $P < 0.01$, *** $P < 0.001$.

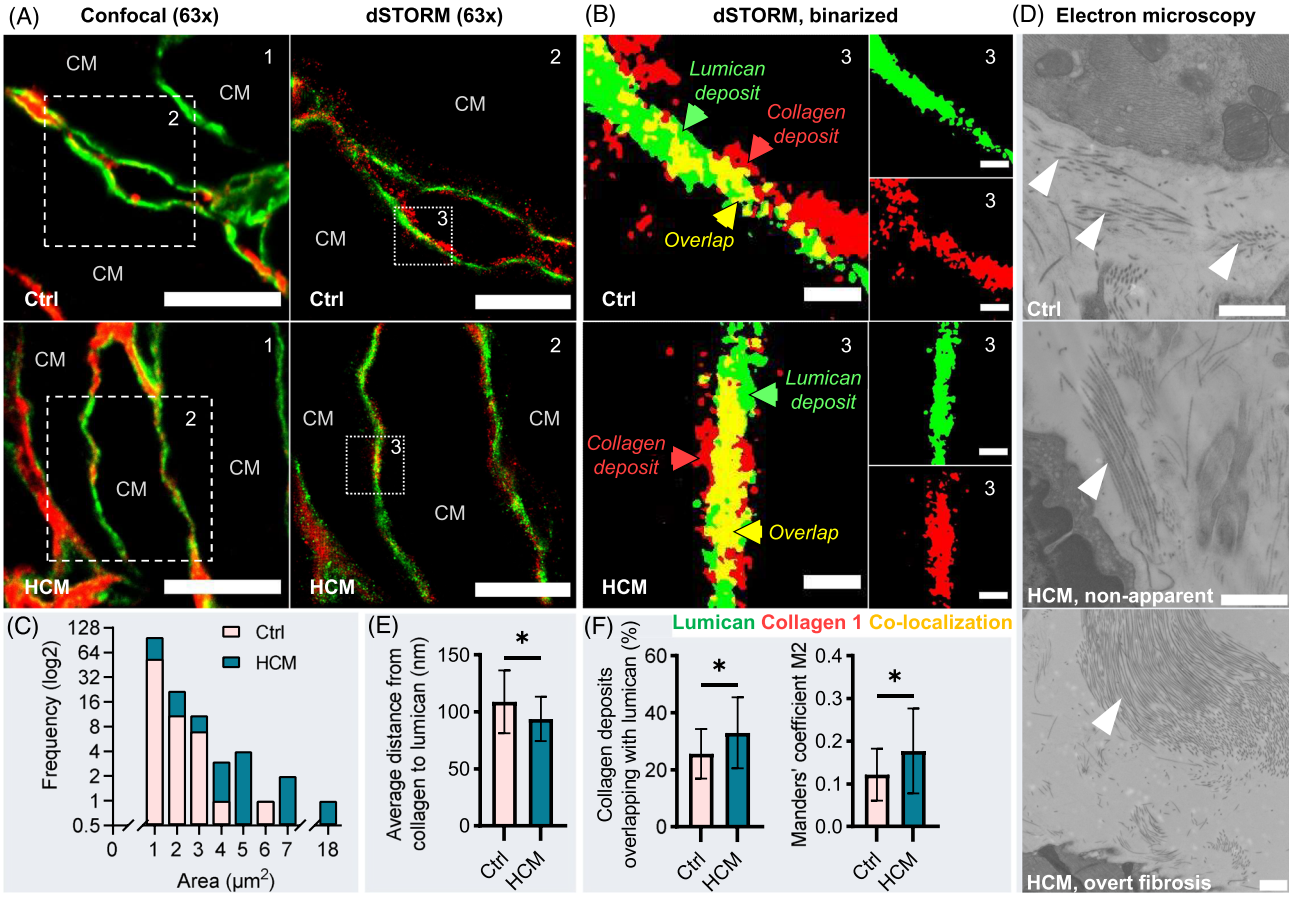

understanding, we must first thoroughly examine key players in the ECM. Our findings contribute to this gap by thoroughly assessing lumican in fibrosis in HCM, describing its clear co-localization with collagen I and identifying that it may act to promote collagen fibril accumulation in this setting. From these findings, we speculate that a therapeutic strategy targeting lumican could attenuate fibrosis when used in combination with a drug targeting hypercontractility, such as mavacamten.

Previous studies in lumican knock-out mice provided important initial insights into lumican's role in cardiac fibrosis. Lumican knock-out mice with pressure overload experienced extreme LV dilatation, attributed to alterations in collagen,[13] whereas heterozygous lumican knock-out mice (50% reduction in lumican gene expression) experienced attenuated fibrotic remodelling.[26] Lumican's effects on cardiomyocyte hypertrophy have been studied previously, where lack of lumican was thought to alter collagen organization in the

DOI: 10.1002/ehf2.14234

Figure 6 Exogenous lumican increases collagen fibre width in cultured human foetal cardiac fibroblasts. Confocal imaging of lumican (green) and collagen I (red) in human foetal cardiac fibroblasts (hfCFBs) cultured for 5 days with recombinant lumican (Lum) or vehicle (Veh), $n = 3$ biological replicates. (A) Representative confocal images of collagen I fibres (right panels, red), lumican (middle panels, green) and merged image (left panels). DAPI (light blue) displays cell nuclei. Seven images were chosen at random from each culture for quantification. Negative antibody control displayed in *Figure S1C*. Scale bar indicates a width of 100 μm. (B) Mean width of all collagen fibres in images. (C) Mean length of all collagen fibres in images. (D) The average number of collagen fibres in images. All data are shown as mean ± SD; statistical comparisons performed by *t*-test. * $P < 0.05$, ** $P < 0.01$, *** $P < 0.001$.

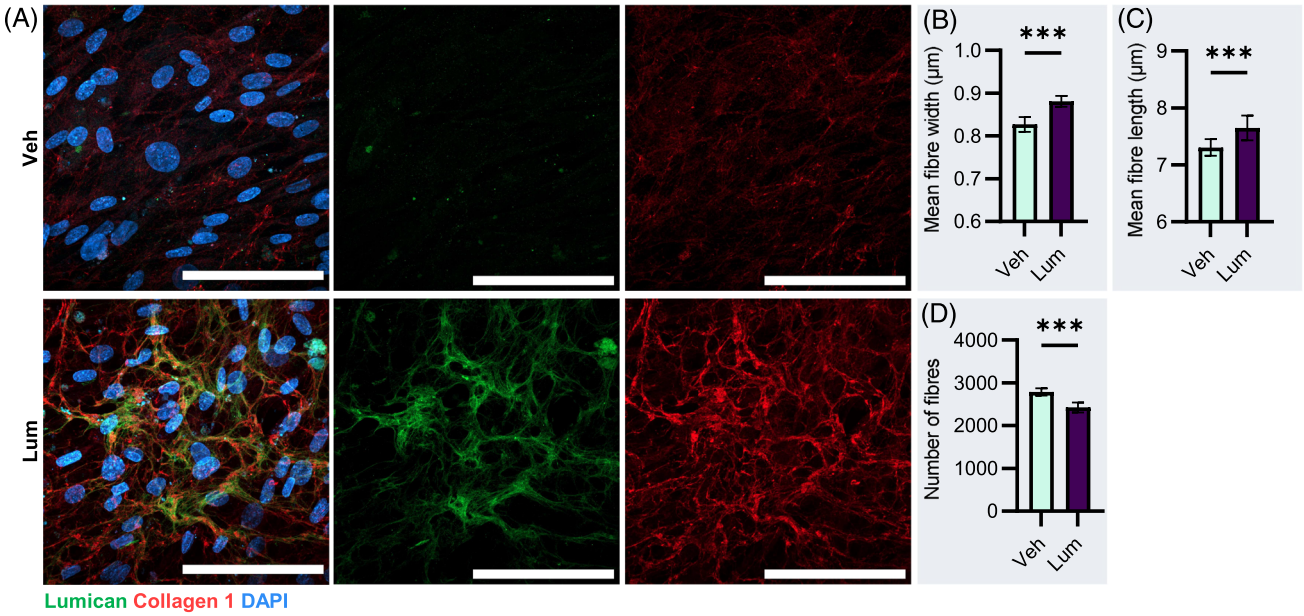

pericellular ECM, and hence the biomechanical properties of the cardiac tissue, causing a hypertrophic response.[12] These findings suggest that disrupting the balance of lumican in the myocardium can have important secondary effects and that lumican plays a critical role in maintaining the structural integrity of cardiac tissue. Our study also indicates that this role in structural integrity arises through fibrillar collagen organization, potentially through regulating the thickness of collagen fibres, as demonstrated in the cornea in pioneer studies of lumican.[34–36] As lumican can bind to collagen I through leucine-rich repeats 5–7, it is possible that lumican's ability to influence collagen fibre formation could be through direct interaction.[30,31] Other studies also indicate that lumican may have a profibrotic role in cardiac diseases and could induce collagen production,[10,13] yet we have not provided data on this role here.

The *Myh6* R403Q mouse model has been instrumental in preclinical studies of HCM.[20,22] By examining tissues from the *Myh6* R403Q mouse model, we were able to expand the scope of our study to examine fibrotic remodelling in detail across an entire LV. By examining patient tissue alone, we were restricted to end-stage, regional septal biopsies derived from a variable control cohort. Therefore, using this mouse model ensures our results are robust when examining subtle alterations in ECM remodelling, as we have performed with dSTORM. However, whole sections could also be examined by defining regions that have undergone similar levels of fibrotic remodelling in order to understand whether lumican is most relevant to a specific stage of fibrosis.

Using dSTORM to generate super-resolution images of the ECM in cardiac tissue and to quantify protein deposition are novel applications of the method. dSTORM itself is a relatively new technique,[37] and, to date, it has only been used to describe ECM in kidney tissue.[38] We believe that applying dSTORM in the cardiac ECM, as we have for lumican and collagen, will facilitate further research into how critical ECM proteins initially or subtly remodel in cardiac fibrosis. Such an application will be relevant to cardiac fibrosis across the field of heart failure, not just in HCM.

One of the limitations to our study, however, is that we were unable to apply dSTORM to examine details within areas of severe fibrotic remodelling, due to saturation of signal. We were therefore unable to provide an in-depth assessment of the relationship between lumican and collagen in areas of severe fibrosis, when thick collagen fibres are already present. Similarly, it was beyond the scope of this study to examine how lumican co-localization with collagen I causes thickening of collagen fibres. Future studies should aim to

elucidate whether increased lumican impacts collagen fibre macrostructure in cardiac tissue via mechanisms previously highlighted in lumican-deficient mice, for example, through alterations to collagen fibril diameter.[12] Regardless, we believe our assessment provides a strong starting point for upcoming studies that wish to define, and perhaps utilize, this molecular mechanism of cardiac fibrosis in HCM.

In conclusion, the importance of proteoglycans in ECM remodelling in heart failure is becoming increasingly demonstrated.[9,39,40] In this study, we have provided the first detailed description of lumican in HCM at a molecular level. We located increased levels of lumican to fibrotic areas and displayed lumican's co-localization with fibrillar collagen. We have also used a novel application of dSTORM imaging to super-resolve the cardiac ECM, observing co-localization and subtle alterations in areas even without overt fibrosis. We suggest that this co-localization of lumican promotes collagen fibril accumulation and hence the formation of thicker collagen fibres. Such a role would directly affect such tissue properties as tensile strength and stiffness,[29] properties that determine diastolic function and are therefore of clinical importance in HCM. In conclusion, we identify lumican is an ECM protein of interest that could hold potential for therapeutic regulation of collagen fibres in fibrosis in HCM.

Acknowledgements

We are grateful to our technicians and animal facility staff, especially Hege Ugland and Marita Martinsen. Hong Qu at NORBRAIN (University of Oslo) acquired numerous excellent tissue section scans. The Core Facility for Advanced Electron Microscopy at Oslo University Hospital provided expert assistance and images from electron microscopy. Our thanks to Debbie Maizels at Zoobotanica for her assistance with scientific illustration.

Conflict of interest

None declared.

Funding

This work was supported by the Norwegian Health Association, the Research Council of Norway, Anders Jahre's Fund for the Promotion of Science, the South-Eastern Norway Regional Health Authority, the Kristian Gerhard Jebsen Foundation, and the Olav Raagholt and Gerd Meidel Raagholt's Fund for Science, Norway.

Supporting information

Additional supporting information may be found online in the Supporting Information section at the end of the article.

Data S1. Supporting Information

Figure S1. Lumican immunostaining of individual patient tissues and negative antibody controls. Complete data for immunohistochemistry in tissues and cell cultures. (A) Representative images of HOCM patient tissue immunostained with an antibody-negative control buffer (goat serum + rabbit IgG), revealing any nonspecific binding of secondary antibodies. WGA (cyan) has been used to indicate presence of ECM, while DAPI (light blue) displays nuclei. The scale bar indicates a width of 250 μm. (B) Representative images of HCM mouse tissues (R403Q + CsA) immunostained with an antibody-negative control buffer (goat serum + rabbit IgG), revealing any nonspecific binding of secondary antibodies. WGA (cyan) has been used to indicate presence of ECM, while DAPI (light blue) displays nuclei. The scale bar indicates a width of 250 μm. (C) Representative images of human foetal cardiac fibroblast cultures immunostained with an antibody-negative control buffer (goat serum + rabbit IgG), controlling for nonspecific binding of secondary antibodies. DAPI (light blue) displays nuclei. The scale bar indicates a width of 100 μm. (D) Patient tissues stained for lumican (green) via immunohistochemistry are displayed in addition to the representative images displayed in Fig. 1B (n = 3). These images were quantified as part of Fig. 1C. The scale bar indicates a width of 1 mm.

Figure S2. Complete lumican Western blots with loading controls for patient cohorts. Complete Western blots displaying lumican protein for all patient samples with associated total protein loading controls (via Coomassie blue) represented and quantified in Fig. 1D. (A) Western blots of control (Ctrl) and HOCM patient samples where lumican protein remains in its native glycosylated state (non-processed). (B) Western blots of control (Ctrl) and HOCM patient samples where lumican protein has been deglycosylated with PNGaseF for further quantification (as described in Fig. 1D). "Ctrl*" = samples omitted from analyses due to poor quality.

Figure S3. HOCM patient circulating biomarker data correlated with lumican protein levels. Levels of myocardial lumican protein determined via Western blotting (deglycosylated protein via processing with PNGaseF) were correlated with serum levels of fibrosis biomarkers in HOCM patients (n = 13–14). (A) Serum amino terminal peptide of type I procollagen (PINP, left panel) and serum carboxy-terminal telopeptide of type I collagen (ICTP, right panel), i.e., biomarkers of fibrosis through collagen I, correlated with levels of myocardial lumican. R^2 and p values displayed within the graph. (B) Serum amino terminal peptide of type III procollagen (PIIINP) i.e., biomarker of fibrosis through collagen III, correlated with levels of myocardial lumican. R^2 and p values displayed within the graph.

Figure S4. Complete lumican Western blots with loading controls for mouse cohorts. Complete Western blots displaying lumican protein for all mouse samples with associated total protein loading controls, represented and quantified in Fig. 3D. Lumican blotting is displayed on the left, with total protein in the same gel displayed on the right. For each individual, the left lane contains cellular, membrane and soluble/loosely-bound ECM protein (cell+sol. ECM) and the right lane contains insoluble and ECM-bound protein (insol. ECM).

Figure S5. Reconstruction of lumican and collagen co-localization in control mouse tissues using 3D dSTORM. Reconstruction of typical lumican and collagen co-localization as viewed via 3D dSTORM in interstitial areas without overt fibrosis in control (WT Veh) mouse tissue. Collagen localization was obtained with dSTORM imaging and lumican location obtained via confocal imaging. Colour scalars on the right-hand side display colour 'heatmap' used to visualise density of collagen (lower scalar; blue-white = least dense signal and red = most dense signal) and lumican (upper scalar; purple = least dense signal and yellow-green = most dense signal). On the left-hand side, X (red), Y (yellow) and Z (green) axis arrows display orientation during rotation with scale bar displaying 1 μm.

Figure S6. Reconstruction of lumican and collagen co-localization in HCM mouse tissues using 3D dSTORM. Reconstruction of typical lumican and collagen co-localization as viewed via 3D dSTORM in interstitial areas without overt fibrosis in HCM (*Myh6* R403Q + CsA) mouse tissue. Collagen localization was obtained with dSTORM imaging and lumican location obtained via confocal imaging. Colour scalars on the right-hand side display colour 'heatmap' used to visualise density of collagen (lower scalar; blue-white = least dense signal and red = most dense signal) and lumican (upper scalar; purple = least dense signal and yellow-green = most dense signal). On the left-hand side, X (red), Y (yellow) and Z (green) axis arrows display orientation during rotation with scale bar displaying 1 μm.

References

1. Authors/Task Force members, Elliott PM, Anastasakis A, Borger MA, Borggrefe M, Cecchi F, Charron P, Hagege AA, Lafont A, Limongelli G, Mahrholdt H, McKenna W, Mogensen J, Nihoyannopoulos P, Nistri S, Pieper PG, Pieske B, Rapezzi C, Rutten FH, Tillmanns C, Watkins H. 2014 ESC guidelines on diagnosis and management of hypertrophic cardiomyopathy: The task force for the diagnosis and management of hypertrophic cardiomyopathy of the European Society of Cardiology (ESC). *Eur Heart J*. 2014; **35**: 2733–2779.
2. Marian AJ, Braunwald E. Hypertrophic cardiomyopathy: Genetics, pathogenesis, clinical manifestations, diagnosis, and therapy. *Circ Res*. 2017; **121**: 749–770.
3. Maron BJ, Roberts WC, Epstein SE. Sudden death in hypertrophic cardiomyopathy: A profile of 78 patients. *Circulation*. 1982; **65**: 1388–1394.
4. O'Hanlon R, Grasso A, Roughton M, Moon JC, Clark S, Wage R, Webb J, Kulkarni M, Dawson D, Sulaibeekh L, Chandrasekaran B, Bucciarelli-Ducci C, Pasquale F, Cowie MR, McKenna WJ, Sheppard MN, Elliott PM, Pennell DJ, Prasad SK. Prognostic significance of myocardial fibrosis in hypertrophic cardiomyopathy. *J Am Coll Cardiol*. 2010; **56**: 867–874.
5. Raman B, Ariga R, Spartera M, Sivalokanathan S, Chan K, Dass S, Petersen SE, Daniels MJ, Francis J, Smillie R, Lewandowski AJ, Ohuma EO, Rodgers C, Kramer CM, Mahmod M, Watkins H, Neubauer S. Progression of myocardial fibrosis in hypertrophic cardiomyopathy: Mechanisms and clinical implications. *Eur Heart J Cardiovasc Imaging*. 2019; **20**: 157–167.
6. Almaas VM, Haugaa KH, Strøm EH, Scott H, Dahl CP, Leren TP, Geiran OR, Endresen K, Edvardsen T, Aakhus S, Amlie JP. Increased amount of interstitial fibrosis predicts ventricular arrhythmias, and is associated with reduced myocardial septal function in patients with obstructive hypertrophic cardiomyopathy. *EP Europace*. 2013; **15**: 1319–1327.
7. González A, Schelbert EB, Díez J, Butler J. Myocardial interstitial fibrosis in heart failure: Biological and translational perspectives. *J Am Coll Cardiol*. 2018; **71**: 1696–1706.
8. López B, Querejeta R, González A, Larman M, Díez J. Collagen cross-linking but not collagen amount associates with elevated filling pressures in hypertensive patients with stage C heart failure. *Hypertension*. 2012; **60**: 677–683.
9. Christensen G, Herum KM, Lunde IG. Sweet, yet underappreciated: proteoglycans and extracellular matrix remodeling in heart disease. *Matrix Biol*. 2019; **75-76**: 286–299.
10. Engebretsen KV, Lunde IG, Strand ME, Waehre A, Sjaastad I, Marstein HS, Skrbic B, Dahl CP, Askevold ET, Christensen G, Bjørnstad JL, Tønnessen T. Lumican is increased in experimental and clinical heart failure, and its production by cardiac fibroblasts is induced by mechanical and proinflammatory stimuli. *FEBS J*. 2013; **280**: 2382–2398.
11. Coats CJ, Heywood WE, Virasami A, Ashrafi N, Syrris P, dos Remedios C, Treibel TA, Moon JC, Lopes LR, McGregor CGA, Ashworth M, Sebire NJ, McKenna WJ, Mills K, Elliott PM. Proteomic analysis of the myocardium in hypertrophic obstructive cardiomyopathy. *Circ Genom Precis Med*. 2018; **11**: e001974.
12. Dupuis LE, Berger MG, Feldman S, Doucette L, Fowlkes V, Chakravarti S, Thibaudeau S, Alcala NE, Bradshaw AD, Kern CB. Lumican deficiency results in cardiomyocyte hypertrophy with altered collagen assembly. *J Mol Cell Cardiol*. 2015; **84**: 70–80.
13. Mohammadzadeh N, Lunde IG, Andenæs K, Strand ME, Aronsen JM, Skrbic B, Marstein HS, Bandlien C, Nygård S, Gorham J, Sjaastad I, Chakravarti S, Christensen G, Engebretsen KVT, Tønnessen T. The extracellular matrix proteoglycan lumican improves survival and counteracts cardiac dilatation and failure in mice subjected to pressure overload. *Sci Rep*. 2019; **9**: 9206.
14. Krishnan A, Li X, Kao WY, Viker K, Butters K, Masuoka H, Knudsen B, Gores G, Charlton M. Lumican, an extracellular matrix proteoglycan, is a novel requisite for hepatic fibrosis. *Lab Invest*. 2012; **92**: 1712–1725.
15. Zhou B, Tu T, Gao Z, Wu X, Wang W, Liu W. Impaired collagen fibril assembly in keloids with enhanced expression of lumican and collagen V. *Arch Biochem Biophys*. 2021; **697**: 108676.

16. Xiao D, Liang T, Zhuang Z, He R, Ren J, Jiang S, Zhu L, Wang K, Shi D. Lumican promotes joint fibrosis through TGF-β signaling. *FEBS Open Bio*. 2020; **10**: 2478–2488.
17. Percie du Sert N, Ahluwalia A, Alam S, Avey MT, Baker M, Browne WJ, Clark A, Cuthill IC, Dirnagl U, Emerson M, Garner P, Holgate ST, Howells DW, Hurst V, Karp NA, Lazic SE, Lidster K, MacCallum CJ, Macleod M, Pearl EJ, Petersen OH, Rawle F, Reynolds P, Rooney K, Sena ES, Silberberg SD, Steckler T, Würbel H. Reporting animal research: Explanation and elaboration for the ARRIVE guidelines 2.0. *PLoS Biol*. 2020; **18**: e3000411.
18. Geisterfer-Lowrance AA, Christe M, Conner DA, Ingwall JS, Schoen FJ, Seidman CE, Seidman JG. A mouse model of familial hypertrophic cardiomyopathy. *Science*. 1996; **272**: 731–734.
19. Fatkin D, McConnell BK, Mudd JO, Semsarian C, Moskowitz IG, Schoen FJ, Giewat M, Seidman CE, Seidman JG. An abnormal Ca(2+) response in mutant sarcomere protein-mediated familial hypertrophic cardiomyopathy. *J Clin Invest*. 2000; **106**: 1351–1359.
20. Teekakirikul P, Eminaga S, Toka O, Alcalai R, Wang L, Wakimoto H, Nayor M, Konno T, Gorham JM, Wolf CM, Kim JB, Schmitt JP, Molkentin JD, Norris RA, Tager AM, Hoffman SR, Markwald RR, Seidman CE, Seidman JG. Cardiac fibrosis in mice with hypertrophic cardiomyopathy is mediated by non-myocyte proliferation and requires Tgf-β. *J Clin Invest*. 2010; **120**: 3520–3529.
21. Sjaastad I, Sejersted OM, Ilebekk A, Bjornerheim R. Echocardiographic criteria for detection of postinfarction congestive heart failure in rats. *J Appl Physiol (1985)*. 2000; **89**: 1445–1454.
22. Green EM, Wakimoto H, Anderson RL, Evanchik MJ, Gorham JM, Harrison BC, Henze M, Kawas R, Oslob JD, Rodriguez HM, Song Y, Wan W, Leinwand LA, Spudich JA, McDowell RS, Seidman JG, Seidman CE. A small-molecule inhibitor of sarcomere contractility suppresses hypertrophic cardiomyopathy in mice. *Science*. 2016; **351**: 617–621.
23. Chen D, Smith LR, Khandekar G, Patel P, Yu CK, Zhang K, Chen CS, Han L, Wells RG. Distinct effects of different matrix proteoglycans on collagen fibrillogenesis and cell-mediated collagen reorganization. *Sci Rep*. 2020; **10**: 19065.
24. Karamanou K, Franchi M, Piperigkou Z, Perreau C, Maquart FX, Vynios DH, Brézillon S. Lumican effectively regulates the estrogen receptors-associated functional properties of breast cancer cells, expression of matrix effectors and epithelial-to-mesenchymal transition. *Sci Rep*. 2017; **7**: 45138.
25. Naba A, Clauser KR, Hynes RO. Enrichment of extracellular matrix proteins from tissues and digestion into peptides for mass spectrometry analysis. *J Vis Exp*. 2015; **101**: e53057.
26. Mohammadzadeh N, Melleby AO, Palmero S, Sjaastad I, Chakravarti S, Engebretsen KVT, Christensen G, Lunde IG, Tønnessen T. Moderate loss of the extracellular matrix proteoglycan lumican attenuates cardiac fibrosis in mice subjected to pressure overload. *Cardiology*. 2020; **145**: 187–198.
27. Chen S-W, Tung Y-C, Jung S-M, Chu Y, Lin P-J, Kao WWY, Chu PH. Lumican-null mice are susceptible to aging and isoproterenol-induced myocardial fibrosis. *Biochem Biophys Res Commun*. 2017; **482**: 1304–1311.
28. Engebretsen KV, Waehre A, Bjørnstad JL, Skrbic B, Sjaastad I, Behmen D, Marstein HS, Yndestad A, Aukrust P, Christensen G, Tønnessen T. Decorin, lumican, and their GAG chain-synthesizing enzymes are regulated in myocardial remodeling and reverse remodeling in the mouse. *J Appl Physiol*. 2013; **114**: 988–997.
29. Chakravarti S, Magnuson T, Lass JH, Jepsen KJ, LaMantia C, Carroll H. Lumican regulates collagen fibril assembly: Skin fragility and corneal opacity in the absence of lumican. *J Cell Biol*. 1998; **141**: 1277–1286.
30. Kalamajski S, Oldberg Å. Homologous sequence in lumican and fibromodulin leucine-rich repeat 5-7 competes for collagen binding. *J Biol Chem*. 2009; **284**: 534–539.
31. Svensson L, Närlid I, Oldberg Å. Fibromodulin and lumican bind to the same region on collagen type I fibrils. *FEBS Lett*. 2000; **470**: 178–182.
32. Saberi S, Cardim N, Yamani M, Schulz-Menger J, Li W, Florea V, Sehnert AJ, Kwong RY, Jerosch-Herold M, Masri A, Owens A, Lakdawala NK, Kramer CM, Sherrid M, Seidler T, Wang A, Sedaghat-Hamedani F, Meder B, Havakuk O, Jacoby D. Mavacamten favorably impacts cardiac structure in obstructive hypertrophic cardiomyopathy: EXPLORER-HCM cardiac magnetic resonance substudy analysis. *Circulation*. 2021; **143**: 606–608.
33. Sewanan LR, Schwan J, Kluger J, Park J, Jacoby DL, Qyang Y, Campbell SG. Extracellular matrix from hypertrophic myocardium provokes impaired twitch dynamics in healthy cardiomyocytes. *JACC Basic Transl Sci*. 2019; **4**: 495–505.
34. Chakravarti S. Functions of lumican and fibromodulin: Lessons from knockout mice. *Glycoconj J*. 2002; **19**: 287–293.
35. Rada JA, Cornuet PK, Hassell JR. Regulation of corneal collagen fibrillogenesis in vitro by corneal proteoglycan (lumican and decorin) core proteins. *Exp Eye Res*. 1993; **56**: 635–648.
36. Chakravarti S, Zhang G, Chervoneva I, Roberts L, Birk DE. Collagen fibril assembly during postnatal development and dysfunctional regulation in the lumican-deficient murine cornea. *Dev Dyn*. 2006; **235**: 2493–2506.
37. Endesfelder U, Heilemann M. Direct stochastic optical reconstruction microscopy (dSTORM). *Methods Mol Biol*. 2015; **1251**: 263–276.
38. Suleiman H, Zhang L, Roth R, Heuser JE, Miner JH, Shaw AS, Dani A. Nanoscale protein architecture of the kidney glomerular basement membrane. *Elife*. 2013; **2**: e01149-e.
39. Frangogiannis NG. The extracellular matrix in myocardial injury, repair, and remodeling. *J Clin Invest*. 2017; **127**: 1600–1612.
40. Rienks M, Papageorgiou AP, Frangogiannis NG, Heymans S. Myocardial extracellular matrix: An ever-changing and diverse entity. *Circ Res*. 2014; **114**: 872–888.